Two-photon intravital imaging of thrombus development

Malgorzata M. Kamocka
Indiana University School of Medicine
Department of Medical and Molecular Genetics
975 West Walnut Street
IB130
Indianapolis, Indiana 46202
and
Indiana Center for Vascular Biology and Medicine
975 West Walnut Street
IB 441
Indianapolis, Indiana 46202

Jian Mu
Xiaomin Liu
University of Notre Dame
Department of Computer Science and Engineering
384 Fitzpatrick Hall
Notre Dame, Indiana 46556

Nan Chen
University of Texas
M.D. Anderson Cancer Center
1515 Holcombe Boulevard
Houston, Texas 77030

Amy Zollman
Indiana University School of Medicine
Department of Medical and Molecular Genetics
975 West Walnut Street
IB130
Indianapolis, Indiana 46202
and
Indiana Center for Vascular Biology and Medicine
975 West Walnut Street
IB 441
Indianapolis, Indiana 46202

Barbara Sturonas-Brown
Kenneth Dunn
Indiana University School of Medicine
Indiana Center for Biological Microscopy
950 West Walnut Street
R2 Suite 233
Indianapolis, Indiana 46202

Zhiliang Xu
University of Notre Dame
Department of Mathematics
Interdisciplinary Center for the Study of Biocomplexity
255 Hurley Hall
Notre Dame, Indiana 46556

Danny Z. Chen
University of Notre Dame
Department of Computer Science and Engineering
384 Fitzpatrick Hall
Notre Dame, Indiana 46556

Mark S. Alber
University of Notre Dame
Department of Mathematics
Interdisciplinary Center for the study of Biocomplexity
255 Hurley Hall
Notre Dame, Indiana 46556

Elliot D. Rosen
Indiana University School of Medicine
Department of Medical and Molecular Genetics
975 West Walnut Street
IB130
Indianapolis, Indiana 46202
and
Indiana Center for Vascular Biology and Medicine
975 West Walnut Street
IB 441
Indianapolis, Indiana 46202

Address all correspondence to: Malgorzata Kamocka, Indiana University School of Medicine, 975 West Walnut St. IB-130, Indianapolis, IN 46202 Tel: 317 274-2274; Fax: 317 278-0130; E-mail: E-mail: mkamocka@iupui.edu

Abstract. Thrombus development in mouse mesenteric vessels following laser-induced injury was monitored by high-resolution, near-real-time, two-photon, intravital microscopy. In addition to the use of fluorescently tagged fibrin(ogen) and platelets, plasma was labeled with fluorescently tagged dextran. Because blood cells exclude the dextran in the single plane, blood cells appear as black silhouettes. Thus, in addition to monitoring the accumulation of platelets and fibrin in the thrombus, the protocol detects the movement and incorporation of unlabeled cells in and around it. The developing thrombus perturbs the blood flow near the thrombus surface, which affects the incorporation of platelets and blood cells into the structure. The hemodynamic effects and incorporation of blood cells lead to the development of thrombi with heterogeneous domain structures. Additionally, image processing algorithms and simulations were used to quantify structural features of developing thrombi. This analysis suggests a novel mechanism to stop the growth of developing thrombus. [DOI: 10.1117/1.3322676]

Keywords: thrombogenesis; coagulation; hemostasis; laser vascular injury; two-photon imaging; intravital microscopy.

Paper 08453R received Dec. 30, 2008; revised manuscript received Nov. 2, 2009; accepted for publication Dec. 18, 2009; published online Feb. 23, 2010.

1 Introduction

Although the hemostatic system has evolved to rapidly form a clot to stop hemorrhage following injury, the response must be regulated to avoid pathological thrombus formation blocking blood flow within vessels. The importance of controlling the response is underscored by the high rate of thrombosis requiring hospitalization each year. For instance ~0.1% of the population develops symptomatic deep vein thrombosis (DVT) each year in the U.S.[1,2] one in 20 people will suffer

1083-3668/2010/15(1)/016020/7/$25.00 © 2010 SPIE

DVT in their lifetime. There are ~100,000 deaths due to pulmonary embolism, caused by dislodged thrombus fragments trapped in the pulmonary circulation.

Our understanding of the processes involved in thrombus development has advanced in the last decade as a result of the availability of genetically engineered mice with deficiencies of hemostatic components. Additionally, technical advances have enabled scientists to better monitor thrombogenesis. For instance, the use of intravital microscopy allows one to record early events in thrombus development in real time, enabling one to characterize this dynamic process. Many different experimental systems have been established in different animal models, using different vessels, different injury protocols, and different monitoring modalities.[3–26]

One of the more exciting recent developments has been the use of fluorescent intravital video microscopy.[27–30] Using fluorescent probes for different hemostatic factors, it is possible to monitor the incorporation of different thrombus components. In 2002, Falati et al.[5] described the use of an intravital microscopic system to monitor three fluorescent channels simultaneously in real time. Monitoring thrombus development with these techniques in mice with hemostatic deficiencies has provided new insights into the role of particular components in thrombogenesis.

We have modified the protocol described by Falati et al.[5] by using two-photon intravital microscopy to record thrombogenesis in a single optical plane. In addition to fluorescently tagging fibrin(ogen) and platelets, we used fluorescently labeled dextran to detect plasma.

Imaging data can be collected in two modes. The first includes taking continuous images at a single image plane generating near-real-time movies of a single cross section through the thrombus. Because cells in blood exclude the labeled dextran, they appear as "black holes" enabling one to track flow around the thrombus. The second mode involves generating sequential Z stacks through the developing thrombus enabling one to generate high-resolution structural information. Image-processing algorithms developed by Mu et al.[31,32] allow one to quantify properties of the developing thrombus. Contiguous segments of the thrombus that exclude all fluorophores, and thus appear black, are included in the thrombus as domains containing something other than fibrin(ogen) and/or platelets. Given the shape and size of some of the black segments, they include leukocytes and erythrocytes. However, the acquisition of high-resolution spatial information sacrifices temporal resolution because the time interval required to collect images to generate a 3-D structure is of the order of 1 min.

2 Materials and Methods

2.1 *Mice*

C57Bl/5 mice, 6–8 weeks of age were used in accordance with NIH guidelines and approval of the Institutional Animal Care and Use Committee of the Indiana University School of Medicine.

2.2 *Injury Protocol and Visualization*

After anesthesia with injectable anesthetic (ketamine/xylazine/acepromazine; 8.3 μL/g of body weight), mice were injected with fluorescently labeled probes through tail vein injection and the mesentery was exposed by central incision in the abdomen, permitting visualization of thrombus development in mesenteric venules. The probes used in experiment include (*i*) tetramethyrhodamine-labeled 70,000 MW dextran (Molecular Probes, Eugene, Oregon), or Alexa Fluor 350 (Molecular Probes) labeled 70,000 dextran (Molecular Probes), (*ii*) human fibrinogen (Enzyme Research Laboratories, South Bend, Indiana) labeled with Alexa Fluor 350 (Molecular Probes) or Alexa Fluor 488 tagged human fibrinogen (Molecular Probes), and (*iii*) rat antimouse CD41/61 MAb (Emfret Analytics, Wurzburg, Germany) mixed with secondary goat antirat IgG antibody labeled with Alexa Fluor 488 or 546 (Molecular Probes).

A Zeiss LSM-510 Meta Confocal/Multiphoton microscope system (Zeiss, Jena, Germany) equipped with a tunable titanium-sapphire laser (Spectra—Physics, Mountain View, California) and a 63×/1.2 or 40×/1.2 W Korr ultraviolet-visible-infrared Apochromat objective (Zeiss) at the Indiana Center for Biological Microscopy was used for visualization. Direct laser-induced injuries were made in the mesenteric venules by exposing a small area of the vessel wall to a laser of 20.4-mW power for 10–15 s at 800 nm. Injuries were made using two protocols: (*i*) on the luminal surface at the side of the vessel wall and (*ii*) using advantages of 2P mode, on the luminal surface of the top of the vessel wall. Because the lumen of the vessel was identified by the detection of the labeled dextran probe in blood, one could define the endothelium on the side of vessel wall as a border adjacent to the plasma fluorescent signal. The top luminal surface could be specified by raising the focal plane until one first loses the fluorescent signal from labeled dextran in the blood.

The development of thrombi was monitored by intravital two-photon microscopy at 4 mW, which is not sufficient to generate injury. Because power adjustments are made following injury, the initial frames of the video recording thrombus development occur ~5 s after the induction of injury. The fluorescence was detected by descanned detectors. The emission light was split into three channels to visualize fibrin, platelets, and plasma. The fluorescence was directed through the main dichroic filter HFT KP 650 and three secondary dichroics: NFT545, NFT490 and Plate and then selected by barrier filter bandpass (BP) 555–672 nm in Chs1, BP 390–465 nm in Ch2, and BP 500–550 nm in Ch3. Images were collected at 512×512 pixel resolution, enabling one to capture images at 983 ms/frame speed. The chosen parameters represent a compromise between optical resolution and frame rate by providing sufficient (but not optimal) spatial detail for structural analysis while permitting the acquisition of near-real-time video crucial for monitoring a dynamic process.

Image data were acquired in two modes. Pictures in a single optical plane were collected continuously to reconstruct movies showing high dynamic changes within a cross section of a growing thrombus. The second mode involved the sequential collection of a vertical series of individual optical slices (Z stack) enabling one to generate 3-D reconstructions and perform structural analysis of the developing thrombus.

Processing of images was performed with MetaMorph (Molecular Devices, Downingtown, Pennsylvania) and 3-D reconstructions were made using the Voxx software package[33,34] (Indiana Center for Biological Microscopy, India-

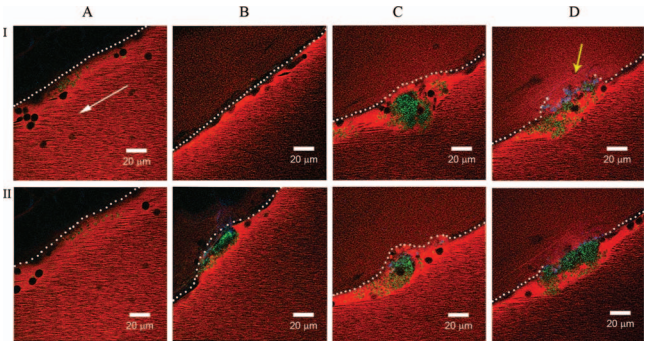

Fig. 1 Laser-induced mesentery thrombi depend upon exposure time. (a–d) show thrombi obtained by using increasing time of laser exposure (5, 10, 15, and 20 s, respectively) at 50 (panel I) and 100 seconds (panel II) after the induction of injury. White dotted line indicates vessel wall, white arrow indicates direction of blood flow in all pictures, and yellow arrow in picture "d" indicated disruption of vessel wall and hemorrhage. Pictures were collected using a 63× objective. Green, platelets; blue, fibrin; red, plasma.

napolis, Indiana). Quantitative measurements of the thrombus were determined using the algorithms described in Mu et al.[31,32]

3 Results

Laser scanning of a single optical plane at 512×512 resolution with the Zeiss LSM-510 Meta Confocal/Multiphoton microscope takes 983 ms, enabling one to make a near-real-time video (1 fps) of a cross section of the developing thrombus. Laser-induced injury is made to a selected region of interest on the luminal side of the vessel wall, which is defined by the region adjacent to the plasma column generated by the dextran signal. Following injury, laser power is reduced to levels that do not induce injury while sequential images are recorded for 20 min.

The extent of injury increases with increased irradiation either by increasing laser power or exposing the region of interest for longer times. Figure 1 shows the effects of increasing laser exposure time during injury using constant power (20.4 mW) in a 150-μm mesenteric venule. Figures 1(a)–1(d) show representative thrombi developed in the vessel while exposed for 5, 10, 15, and 20 s at 20.4 mW laser power captured 50 and 100 s after induction of the injury. Five-second laser exposure is not sufficient to generate a thrombus, while injuries induced by 10 s exposure are highly variable. Exposure for 15 s generates consistent subocclusive thrombi with rare hemorrhage. Longer exposure times increase the size of the injury but increase the incidence of vessel rupture and bleeding.

A feature of this experimental system is that one can visualize slowly moving blood cells in the circulation without specific cell labeling. They appear as "black silhouettes" because the cells exclude the fluorescent signal from fluorescently labeled plasma (dextran) in the focal plane of the two-photon microscopy. Although, we cannot definitively distinguish particular cell types without cell specific staining or exclude other artifacts (such as shredded endothelium excluding dextran from the view), we still can speculate about

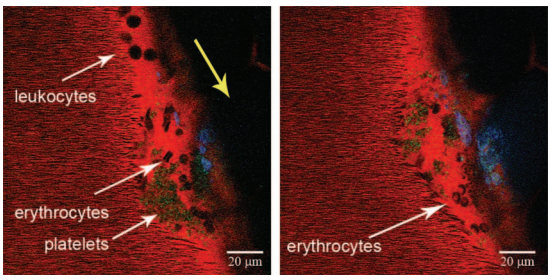

Fig. 2 Unlabeled blood cells appearance in intravital 2P microscopy with labeled plasma. Pictures show silhouettes (black holes) of non-labeled, slowly moving cells along the vessel wall. On the basis of the shape and size of the "black holes" it is likely they represent erythrocytes and leukocytes as indicated. Yellow arrow indicates the direction of blood flow; green, platelets; blue, fibrin; red, plasma; 63× objective was used.

cell type based on observed shape and size (Fig. 2). These flowing black silhouettes of blood cells enable us to detect movement around growing thrombus.

The ability to see silhouettes along the vessel wall means these cells are moving slowly either because they are trapped in vortices or cavities within the clot or due to interactions with the endothelium. In contrast, fast-moving cells appear as horizontal lines because they pass out of the viewing area by the time of the laser scan of the next line.

The images in Fig. 3 show frames from an intravital 2-P video of a developing thrombus induced by 20.4-W laser power for 10 s. As can be seen in the frames, the growth of the thrombus is irregular. Tracking the motion of the slow moving cells, one can detect that the growing thrombus disturbs the flow field causing vortices near the thrombus surface (Video 1). The flow turbulence in turn influences the development of the thrombus. Video 1 indicates that large numbers of blood cells are caught in the vortices forming near the surface of the thrombus and are incorporated into the developing structure. In addition to fibrin(ogen) (blue) and activated platelets (green), the thrombus includes large numbers of blood cells visualized as black silhouettes in plasma (red). Moreover, one can detect clusters of loosely aggregated platelets down stream of the growing structure, which are caught in large vortices and move upstream toward the developing thrombus.

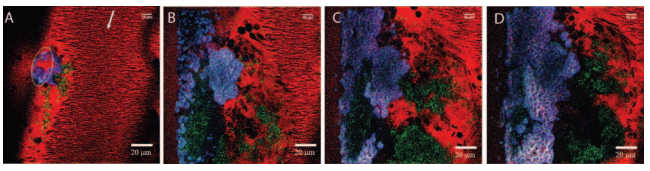

Fig. 3 Intravital 2P images of a developing venous thrombus. (a) shows an early image of the initial state of the thrombus 15 seconds after laser-induced injury (oval indicates site of laser illumination to induce injury). (b–d) shows the status of the thrombus at t=296, t=480, and t=746 s, respectively. In time, the number of activated platelets incorporated in the thrombus increases, a fibrin network develops near the injured vessel wall and blood cells are incorporated into the growing thrombus. The arrow indicates the direction of blood flow; green, platelets; blue, fibrin; red, plasma; 63× objective was used.

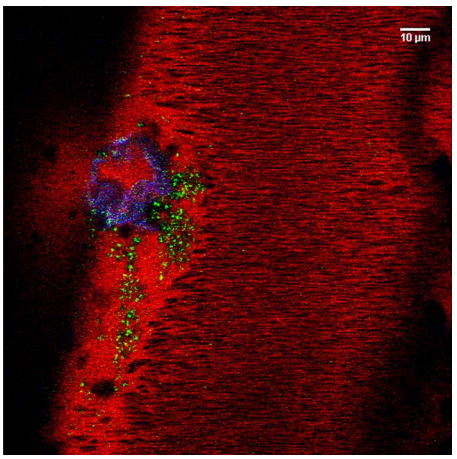

Video 1 Laser-induced thrombus formation. Movie shows an early and late stage of thrombus formation in a mesenteric venule. After laser injury promotion on left side of vessel wall, accumulation of platelets (green) and fibrin (blue) is observed. As the thrombus grows, flow around it becomes turbulent, influencing its shape. Red-labeled plasma allows tracking the movement of unlabeled cells (visible as black silhouettes), which exclude plasma fluorescent signal from plane of view. Data were captured with 63× objective at 512 ×512 pixels resolution. Movie is played 15 times faster then acquired (MPEG, 20.97 MB). [URL: http://dx.doi.org/10.1117/1.3322676.1].

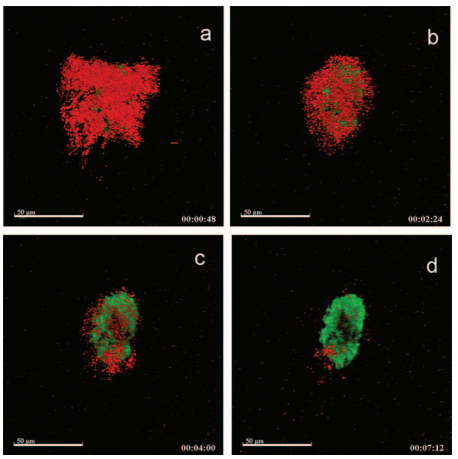

Fig. 4 3D reconstructions of developing mesenteric thrombus. Pictures show luminal view of 3-D reconstructed developing thrombus at four representative time points [48 s, 2 min 24 s, 4 min, and 7 min 12 s; (a) to (d), respectively]. (a, b) represent early time points of thrombus growth while the composition, size, and shape of the thrombus is changing rapidly; (c, d) show of the thrombus after is has stabilized with a fibrin "coat" on its surface. Green, fibrin; red, platelets; 40× objective was used.

In addition to the 2-P video microscopy in one plane, we can also generate a vertical stack of two-photon images that can be compiled to form a 3-D reconstruction of thrombi. With labeled dextran in plasma as one image optical planes approaching the top of the vessel the width of the plasma column in the image plane decreases. The distance of the first plane at which the plasma signal is lost is then less than the distance between image planes from the luminal surface. Thus, using a vertical displacement of 0.45 μm between planes enables us to focus on a plane, including the endothelial cells lining the vessel wall. This strategy enables us to consistently induce laser injury at nearly the same depth of the vessel wall. Furthermore, injuring the top of the vessel and then taking vertical stacks of image cross sections enables us to align the sequential structures, because we can define the base of the thrombus (the first plane we detect a signal) even if there is slight vertical displacement of the vessel. Alignment is much more difficult if one injures the side of the vessel.

Continuous collection of Z stacks following injury enables us to observe how the dynamics of clot structure changes in time. The time to acquire the image stack depends on the resolution of the picture, the distance between image planes and height of the stack. Using parameters enabling us to generate a z stack in ~1 min (512×512 pixels image, of planes spaced 0.45μ m apart of a 30-μm structure) one has a reasonable compromise between spatial and temporal resolution. Figure 4 shows example of 3-D reconstructions of a developing venous thrombus as it changes in time. Images show luminal view of thrombus structures at four time points (48 s, 2 min 24 s, 4 min, and 7 min 12 s). Qualitatively, there is a rapid accumulation of platelets (red) after the induction of injury. Thrombus volume increases rapidly during the first 2 min and then decreases (as a result of platelet contraction) forming a stable structure in 6–10 min. Fibrin is a major component of the stabilized thrombus surface.

Using recently developed image analysis algorithms,[31,32] one can quantify the large collection of image data. Figure 5 shows example of a computer-based reconstruction of a developing thrombus captured at three time points (1, 2, and 6 min after injury promotion). The image-processing algorithms enable us to quantify structural features of developing thrombi. Because thrombus growth occurs on the surface, the changing composition of the surface was analyzed. Algorithms were performed on 16 wild-type injuries. For each injury, a sequence of 3-D images (Z stacks), every 40 s per 3-D image, for a total of 15 Z stacks was produced. Typically, each Z stack consists of about 80 2-D slices. The surface of the thrombus structures formed shortly after injury is primarily composed of voxels consisting of platelets or platelets with fibrin. As the volume of the thrombus stabilizes, the percentage of surface voxels composed of either just fibrin or cells increases and the fraction composed of platelets decreases. Figure 6 shows a graphical representation of the distribution of thrombus components on its surface as a function of distance from the vessel wall (injury site). The surface composition of a developing thrombus shifts from platelet rich to fi-

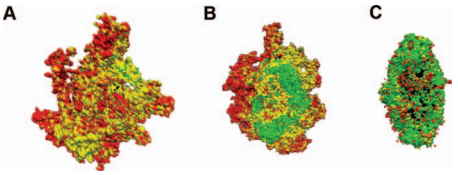

Fig. 5 Computer based 3-D reconstruction of growing thrombus. Pictures show algorithm-based reconstruction of thrombus captured at (a) 1, (b) 2, and (c) 6 min after injury promotion. Green voxels represent fibrin/ogen; red, platelets; yellow, platelets bound fibrin/ogen; and black, unlabeled blood cells.

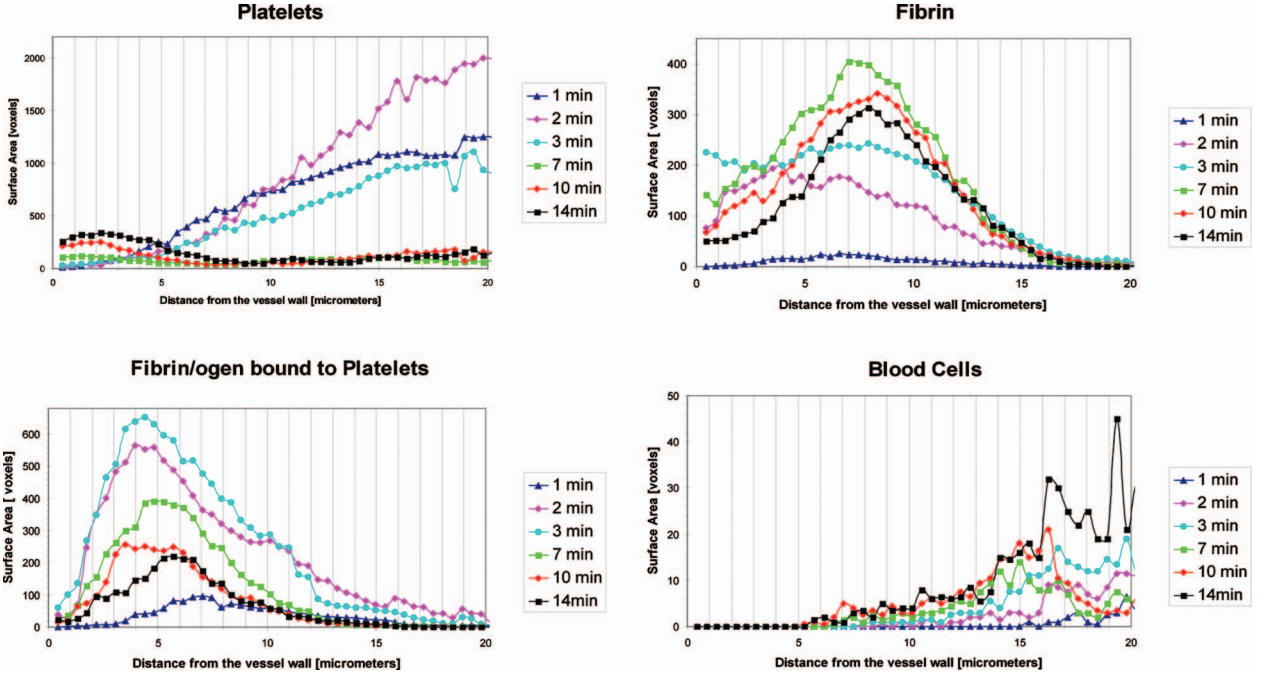

Fig. 6 Composition of thrombus surface at different time points after injury promotion. Graphs show distribution of components on the thrombus surface at six chosen time points (1, 2, 3, 7, 10, and 14 min) as a function of distance from the vessel wall (injury site). Particular thrombus components (platelets, fibrin/ogen, fibrin/ogen bound to platelets, and blood cells) occupy areas at thrombus surface positioned at different distance from the vessel wall. This distribution changes in time. As observed in earlier figures, the surface of the growing thrombus is composed primarily of platelets while that of the stabilized thrombus contains a high percentage of fibrin.

brin as the thrombus shifts from a rapid growth phase to a stable conformation. This suggests the hypothesis that the formation of a fibrin cap on the developing thrombus might limit further thrombus growth.

4 Discussion

Experimental systems utilizing intravital microscopy to monitor thrombus generation *in vivo* following vascular injury have provided new insights into thrombogenesis. Initial protocols recorded video images of vessels generated by light transmission through the vessel. In these systems, the thrombus appears as a white mass developing in the flowing stream. By measuring a cross-sectional area, one can determine the growth of the thrombus. Moreover, the optical density at each pixel in the thrombus image provided some measure of thrombus thickness and/or composition, although the quantitative relationship between optical density and clot thickness *in vivo* is not defined.

The development of multichannel fluorescent imaging techniques has enabled investigators to characterize the accumulation of several components simultaneously in real time. These studies have been extremely informative enabling one to compare the effects of specific hemostatic elements on the temporal and spatial accumulation of thrombus components in real time.

The experimental system described in this report is different from that described in Falati et al.[5] in that thrombus development is monitored by collecting sequential images of a single optical plane. Additionally, one of the channels utilizes fluorescently labeled 70,000 MW dextran to monitor blood. Depending on the resolution and size of the image, the time required to take a single scan is of the order of 1 s. Therefore, it is possible to record data in two modes. The first involves recording from a single optical plane enabling one to generate a near-real-time video of a single cross section of the developing thrombus. The protocol permits monitoring of slow-moving blood cells, which exclude the fluorescent dextran in the focal plane and appear as silhouettes. The second mode involves the continuous collection of vertical z stacks through the thrombus enabling one to collect images for high-resolution structural analysis but with temporal resolution of approximately one structure per minute.

An obvious feature of the near-real-time video is that the blood flow around the growing thrombus is perturbed. As a result of the turbulence and vortices that form behind the thrombus, blood cells and loose platelet aggregates are captured in vortices and get incorporated into the growing thrombus. Of particular interest is that cells and platelet aggregates downstream of the thrombus actually move upstream behind the developing thrombus. As a result, the thrombus structure that forms is highly irregular with different heterogeneous domains.

Although the heterogeneity of thrombi is long known, current hemostatic models of thrombogenesis tend to ignore the observation. However, the heterogeneous domain structure of the clot likely has significant biomedical consequences. The mechanoelastic properties of distinct domains are different. Thus, forces on the clot cause stresses at the interface between domains that may contribute to the formation of emboli.

We have generated a large number of Z stacks of confocal images of the thrombi in the injury models described in this paper. Using the image-processing algorithms it has been pos-

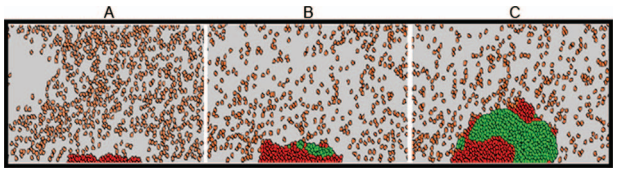

Fig. 7 2-dimentional simulation of thrombus formation in a low shear stress environment. Simulation shows changing structure of growing thrombus captured at early (a), intermediate (b), and late (c) phase of thrombus development. With time, there is a fibrin "cup" (green) developing on the thrombus surface separating procoagulant-activated platelets within the thrombus from zymogens and platelets (red) flowing in blood.

sible to quantify changing structural features of the developing thrombus. In brief, the algorithms set thresholds for each image slice and classify each voxels as either, platelet, fibrin, platelet with fibrin, plasma, or "something else" (corresponding to voxels excluding all fluorophores). The algorithm then defines the thrombus as a contiguous cluster of voxels that are "not plasma" with greater than a threshold volume. Furthermore, the thrombus can then be subdivided into domains of particular composition or of particular positions within the thrombus (such as the surface or at certain distance from the vessel wall). This image analysis suggests that the thrombus undergoes rapid growth within the first 2–3 min after injury and then decreases in volume for the next several minutes, probably as a result of thrombus contraction involving morphological changes of platelets following activation. Interestingly, the thrombus reaches a stable conformation that is characterized by the accumulation of voxels characterized as primarily fibrin on the thrombus surface. This is seen in the 3-D reconstructions generated by the algorithm of Mu et al.[31,32] as well as the graphical representation of thrombus components of the surface as a function of distance from the vessel wall. These conclusions are consistent with the Voxx[33,34] 3-D reconstructions (Fig. 3). These observations suggest a hypothesis that the development of a fibrin "cap" on the developing thrombus may stabilize it by providing structural support for the thrombus but also stops continued growth by separating the prothrombotic surface provided by activated platelets within the clot from resting platelets and coagulation zymogens in the flowing blood.

This hypothesis is consistent with a recently developed computational model developed by Xu et al.[35–37] which predicts that a developing thrombus in a low shear environment (as in a vein) with wild-type levels of coagulation factors develops a surface primarily of fibrin that slows growth. The multiscale model includes processes that are best described as discrete elements and integrates those with processes best described with continuous differential equations. It includes submodels of flow, the formation of polymerized fibrin cells, surface-dependent coagulation reactions, and the interactions of platelets and other blood cells with the developing thrombus. Simulations run using the model suggest that thrombin generated on activated platelets on the thrombus surface promotes further recruitment as well as the formation of fibrin "cells" (Fig. 7).[38] The accumulation of fibrin cells on the surface then separates the procoagulant surface of activated platelets within the thrombus from coagulation zymogens in blood and slows coagulation reactions. Furthermore, resting platelets in blood are less likely to be recruited into the clot because the concentration of platelets activators on the thrombus surface is low due to reduced thrombin generation by platelets within the thrombus and the requirement to diffuse to the surface through fibrin cells.

In summary, the development of the multiphoton imaging protocol described in this paper in which one collects single image planes enables one to develop high-resolution structural information of a developing thrombus although with relatively slow acquisition. The use of recently developed image-processing algorithms enables one to derive structural metrics providing new insights in thrombus development.

Acknowledgments

The work was supported by the Indiana Genetics Initiative (INGEN) and NIH Grant No. HL073750 to EDR; NSF Grant No. DMS-0800612 to MSA, EDR, ZX, MMK, and NC; NSF Grants No. CCF-0515203 and No. CCF-0916606, and NIH Grant No. R01-EB004640 to DZC. None of the authors have a conflict of interest regarding this study.

References

1. G. Cina, R. Marra, C. Di Stasi, and G. Macis, "Epidemiology, pathophysiology and natural history of venous thromboembolism," *Rays* **21**(3), 315–327 (1996).
2. J. A. Heit, "Venous thromboembolism: disease burden, outcomes and risk factors," *Thromb. Haemostasis* **3**(8), 1611–1617 (2005).
3. E. D. Rosen, S. Raymond, A. Zollman, F. Noria, M. Sandoval-Cooper, A. Shulman, J. L. Merz, and F. J. Castellino, "Laser-induced noninvasive vascular injury models in mice generate platelet- and coagulation-dependent thrombi," *Am. J. Pathol.* **158**(5), 1613–1622 (2001).
4. A. Celi, G. Merrill-Skoloff, P. Gross, S. Falati, D. S. Sim, R. Flaumenhaft, B. C. Furie, and B. Furie, "Thrombus formation: direct real-time observation and digital analysis of thrombus assembly in a living mouse by confocal and widefield intravital microscopy," *Thromb. Haemostasis* **1**(1), 60–68 (2003).
5. S. Falati, P. Gross, G. Merrill-Skoloff, B. C. Furie, and B. Furie, "Real-time *in vivo* imaging of platelets, tissue factor and fibrin during arterial thrombus formation in the mouse," *Nat. Med.* **8**(10), 1175–1181 (2002).
6. U. J. Sachs and B. Nieswandt, "*In vivo* thrombus formation in murine models," *Circ. Res.* **100**(7), 979–991 (2007).
7. L. He, L. K. Pappan, D. G. Grenache, Z. Li, D. M. Tollefsen, S. A. Santoro, and M. M. Zutter, "The contributions of the alpha 2 beta 1 integrin to vascular thrombosis *in vivo*," *Blood* **102**(10), 3652–3657 (2003).
8. B. Nieswandt and S. P. Watson, "Platelet-collagen interaction: is GPVI the central receptor?," *Blood* **102**(2), 449–461 (2003).
9. E. J. Weiss, J. R. Hamilton, K. E. Lease, and S. R. Coughlin, "Protection against thrombosis in mice lacking PAR3," *Blood* **100**(9), 3240–3244 (2002).
10. C. Denis, N. Methia, P. S. Frenette, H. Rayburn, M. Ullman-Cullere, R. O. Hynes, and D. D. Wagner, "A mouse model of severe von Willebrand disease: defects in hemostasis and thrombosis," *Proc. Natl. Acad. Sci. U.S.A.* **95**(16), 9524–9529 (1998).
11. P. F. Bodary, "Links between adipose tissue and thrombosis in the mouse," *Arterioscler. Thromb.* **27**(11), 2284–2291 (2007).
12. R. J. Westrick, M. E. Winn, and D. T. Eitzman, "Murine models of vascular thrombosis (Eitzman series)," *Arterioscler. Thromb.* **27**(10), 2079–2093 (2007).
13. D. B. Weinreb, J. G. Aguinaldo, J. E. Feig, E. A. Fisher, and Z. A. Fayad, "Non-invasive MRI of mouse models of atherosclerosis," *NMR Biomed.* **20**(3), 256–264 (2007).
14. B. C. Cooley, C. Y. Chen, and G. Schmeling, "Increased venous versus arterial thrombosis in the Factor V Leiden mouse," *Thromb. Res.* **119**(6), 747–751 (2007).

15. T. J. Verbeuren, "Experimental models of thrombosis and atherosclerosis," *Therapie* **61**(5), 379–387 (2006).
16. X. Wang, P. L. Smith, M. Y. Hsu, D. Gailani, W. A. Schumacher, M. L. Ogletree, and D. A. Seiffert, "Effects of factor XI deficiency on ferric chloride-induced *vena cava* thrombosis in mice," *Thromb. Haemostasis* **4**(9), 1982–1988 (2006).
17. B. Furie and B. C. Furie, "Thrombus formation in a living mouse," *Pathophysiol. Haemost. Thromb.* **35**(1-2), 1–4 (2006).
18. J. O. Deguchi, M. Aikawa, C. H. Tung, E. Aikawa, D. E. Kim, V. Ntziachristos, R. Weissleder, and P. Libby, "Inflammation in atherosclerosis: visualizing matrix metalloproteinase action in macrophages *in vivo*," *Circulation* **114**(1), 55–62 (2006).
19. P. Jagadeeswaran, "Zebrafish: a tool to study hemostasis and thrombosis," *Curr. Opin. Hematol.* **12**(2), 149–152 (2005).
20. D. E. Kim, D. Schellingerhout, F. A. Jaffer, R. Weissleder, and C. H. Tung, "Near-infrared fluorescent imaging of cerebral thrombi and blood-brain barrier disruption in a mouse model of cerebral venous sinus thrombosis," *J. Cereb. Blood Flow Metab.* **25**(2), 226–233 (2005).
21. R. P. Choudhury, V. Fuster, and Z. A. Fayad, "Molecular, cellular and functional imaging of atherothrombosis," *Nat. Rev. Drug Discovery* **3**(11), 913–925 (2004).
22. S. M. Day, J. L. Reeve, D. D. Myers, and W. P. Fay, "Murine thrombosis models [see comment]," *Thromb. Haemostasis* **92**(3), 486–494 (2004).
23. H. Weiler, "Mouse models of thrombosis: thrombomodulin," *Thromb. Haemostasis* **92**(3), 467–477 (2004).
24. N. Mackman, "Mouse models in haemostasis and thrombosis," *Thromb. Haemostasis* **92**(3), 440–443 (2004).
25. R. E. Rumbaut, J. K. Randhawa, C. W. Smith, and A. R. Burns, "Mouse cremaster venules are predisposed to light/dye-induced thrombosis independent of wall shear rate, CD18, ICAM-1, or P-selectin," *Microcirculation (N.Y.)* **11**(3), 239–247 (2004).
26. F. Xu, M. L. Previti, and W. E. Van Nostrand, "Increased severity of hemorrhage in transgenic mice expressing cerebral protease nexin-2/amyloid beta-protein precursor," *Stroke* **38**(9), 2598–2601 (2007).
27. M. B. Kim and I. H. Sarelius, "Distributions of wall shear stress in venular convergences of mouse cremaster muscle," *Microcirculation (N.Y.)* **10**(2), 167–178 (2003).
28. M. B. Kim and I. H. Sarelius, "Role of shear forces and adhesion molecule distribution on P-selectin-mediated leukocyte rolling in postcapillary venules," *Am. J. Physiol. Heart Circ. Physiol.* **287**(6), H2705–2711 (2004).
29. M. A. van Gestel, J. W. Heemskerk, D. W. Slaaf, V. V. Heijnen, S. O. Sage, R. S. Reneman, and M. G. oude Egbrink, "Real-time detection of activation patterns in individual platelets during thromboembolism *in vivo*: differences between thrombus growth and embolus formation," *J. Vasc. Res.* **39**(6), 534–543 (2002).
30. K. Norman, "Techniques: intravital microscopy—a method for investigating disseminated intravascular coagulation?," *Trends Pharmacol. Sci.* **26**(6), 327–332 (2005).
31. J. Mu, X. Liu, M. M. Kamocka, Z. Xu, M. S. Alber, E. D. Rosen, and D. Z. Chen, "Segmentation, reconstruction, and analysis of blood thrombi in 2-photon microscopy images," in *Proc. of 22nd IEEE Symp. on Computer-Based Medical Systems (CBMS)*, Albuquerque (2009).
32. J. Mu, X. Liu, M. M. Kamocka, Z. Xu, M. S. Alber, E. D. Rosen, and D. Z. Chen, "Segmentation, reconstruction, and analysis of blood thrombus formation in 3-D 2-photon microscopy images," *EURASIP J. Appl. Signal Process.* **2010**, 147216 (2010).
33. J. L. Clendenon, C. L. Phillips, R. M. Sandoval, S. Fang, and K. W. Dunn, "Voxx: a PC-based, near real-time volume rendering system for biological microscopy," *Am. J. Physiol.: Cell Physiol.* **282**(1), C213–218 (2002).
34. J. C. Malone, A. F. Hood, T. Conley, J. Nurnberger, L. A. Baldridge, J. L. Clendenon, K. W. Dunn, and C. L. Phillips, "Three-dimensional imaging of human skin and mucosa by two-photon laser scanning microscopy," *J. Cutan Pathol.* **29**(8), 453–458 (2002).
35. Z. Xu, N. Chen, M. M. Kamocka, E. D. Rosen, and M. Alber, "A multiscale model of thrombus development," *J. R. Soc., Interface* **5**(24), 705–722 (2008).
36. Z. Xu, N. Chen, S. C. Shadden, J. E. Marsden, M. M. Kamocka, E. D. Rosen, and M. Alber, "Study of blood flow impact on growth of thrombi using a multiscale model," *Soft Matter* **5**, 769–779 (2009).
37. Z. Xu, J. Mu, X. Liu, M. M. Kamocka, E. D. Rosen, D. Z. A. Chen, and M. S. Alber, "Combined experimental and simulation study of blood clot formation," presented at *Toronto Int. Conf. on Science and Technology for Humanity (TIC-STH)*, Toronto (2009).
38. Z. Xu, J. Mu, X. Liu, M. M. Kamocka, E. D. Rosen, D. Z. A. Chen, and M. S. Alber, "A multiscale model of venous thrombus formation with surface-mediated control of blood coagulation cascade," *Biophys. J.* (in press).